ELSEVIER

Journal of Marine Systems 6 (1995) 87–107

JOURNAL OF MARINE SYSTEMS

A sequential assimilation scheme applied to global wave analysis and prediction

P. Lionello [a], H. Günther [b], B. Hansen [c]

[a] University of Padua, Italy
[b] GKSS, Geesthacht, Germany
[c] ECMWF, Reading, UK

Received 14 September, 1993; revised and accepted 24 January, 1994

Abstract

This paper examines the results of the assimilation of satellite Significant Wave Height (SWH) observations in a global wave prediction model. The model used is the third generation wave model WAM. The assimilation is carried out using a sequential (single time level) scheme. Each assimilation step is split into two parts. The analysed SWH field is built by Optimal Interpolation, and the analysed spectrum is successively derived from it and from the first guess spectrum. The period used in the study is February 1992, and the altimeter data have been provided by the ERS-1 satellite. The results show positive effects of the assimilation on both wave analysis and forecast.

1. Introduction

The third generation wave model WAM (WAMDI Group, 1988) has proven to be an effective tool for wave prediction on a global scale and it is presently used at ECMWF to produce daily five-day forecasts. The main novelty of the model is the absence of restrictions on the shape of the wave spectrum $f(\mathbf{x}, t, \sigma, \theta)$, whose evolution is determined by the input, dissipation and nonlinear source functions (S_{in}, S_{ds}, S_{nl}, respectively), according to the energy transport equation

$$\frac{\partial F}{\partial t} + \nabla(C_g F) = S_{in} + S_{nl} + S_{ds}. \qquad (1)$$

The only constraint on the spectral shape is its extension using an f^{-5} tail at the high frequencies beyond the prognostic range of the model. In the present global operational implementation the wave spectra are computed using 12 directions and 25 logarithmically spaced frequencies covering the range from 0.041 Hz to 0.45 Hz on a 3° resolution grid that extends from 60° South to 69° North.

An efficient data assimilation package, capable of improving the quality of the model products, combining model results and observations, is obviously an important part of a wave prediction system. The data assimilation is not strictly necessary. In fact, while the accuracy of weather prediction depends crucially on the initial conditions, the accuracy of wave prediction depends on the contrary crucially on the quality of the wind fields

0924-7963/95/$09.50
SSDI 0924-7963(94)00010-9

used. This is because the waves disappear when they reach the coast (represented as a fully absorbing boundary) and because they tend to adjust to the wind, growing and reaching under its influence a fully developed state. Therefore, till a few years ago, the emphasis of wave research was on improving the quality of the wave models themselves, and in using a good quality wind field, rather than on data assimilation. Moreover, the presence of only a few reliable wave observations, available in scattered locations generally close to the coasts, was not encouraging for attempting global data assimilation. The launch of oceanographic satellites has completely changed this situation because the instruments mounted on board give a good global coverage of wave data. This offered the opportunity of developing and testing data assimilation schemes. Moreover, the attempts were stimulated by the possibility of using the dependence of waves on wind to derive a wind analysis from a wave analysis, with eventual benefits for weather prediction.

Satellite wave observations are made with the altimeter, which measures the Significant Wave Height (SWH), and with the Synthetic Aperture Radar (SAR), which measures the 2-dimensional wave spectrum. The efforts were initially concentrated on the assimilation of altimeter data. In fact the SAR data could not be used because the software for the fast inversion of the SAR image was not available. Unfortunately the altimeter data are not complete. In fact, they supply the total energy, while the wave dynamics is based on the wave spectrum. Therefore an assimilation scheme that uses only altimeter data has to provide with the analysed spectrum using only its total energy.

Two classes of methods have been proposed for wave assimilation: variational methods and sequential methods — the corresponding methods exist in weather prediction. Variational methods introduce a cost function to quantify the discrepancy between the model and the observations. They determine the solution that minimizes the cost computing its gradient with respect to a chosen set of parameters (generally describing the initial conditions and the wind fields). The assimilation results in a single correction accounting for all the available measurements. Instead, sequential methods combine the observations that are available in the selected time window and the model results at the central time in the window. The assimilation results in a sequence of corrections. None of them considers the previous or later observations, nor the previous and the following results produced by the model. Variational methods are called "multi-time level", because of their capability of simultaneously using the observations available at many different times, whereas sequential methods are called "single-time level". Variational methods are also referred to as dynamic methods, because they use the model dynamics to construct the analysed fields, while sequential methods are referred to as kinematic methods.

The advantages of sequential methods are the simplicity in writing the code and the low computer costs for their application to real situations. The disadvantages are associated with the incompleteness of the wave measurements, which a sequential assimilation scheme is not able to compensate and which forces to formulate "ad hoc" assumptions for the reconstruction of the wave spectrum. The assumptions are of course formulated in the most sensible way, but admittedly they cannot be always satisfactory.

On the contrary variational approaches have high computer costs, they require complicated codes, but they avoid "ad hoc" assumptions, because the model dynamics compensates the incompleteness of the measurements (though this could turn out to be a disadvantage if the dynamics is wrong). The minimization can be carried out with respect to the initial conditions or/and to the control variables. Correspondingly the gradient of the cost function has to be computed with respect to: (i) the variables defining the initial model conditions, (ii) the control variables (e.g. the wind fields), (iii) both the initial conditions and the control variables. Note that the standard WAM model implementation has 300 degrees of freedom in each model grid point (12 directions times 25 frequencies), i.e. there are 300 gradient components for each grid point if the gradient with respect to the initial conditions is required. In spite of the encouraging advancements and the results reported by De Las Heras and Janssen (1993) during this symposium [1] these difficulties has prevented any application to real data till now.

The described results were obtained with a sequential approach that has been developed at ECMWF (Lionello et al., 1992) to use the ERS-1 data as soon as they became available. It is not the first sequential approach that has been developed for wave data assimilation. The subject has a relatively extensive literature: Esteva, 1988; Hasselmann et al., 1988; Janssen et al., 1988; Thomas, 1988; Francis and Stratton, 1990. The scheme used in our study has the following characteristics:

- It modifies both SWH and peak frequency of the wave spectrum, applying a factor to both the energy scale and the frequency scale;
- The factors are different for the windsea and the swell;
- The local wind is corrected where there is windsea;
- O.I. (Optimal Interpolation) is used for producing the analysed SWH fields.

This is, according to our knowledge, the first simulated operational procedure using a wave data assimilation package. Note in particular that the experiment is organized with a series of one-day analysis and five-day forecasts, correspondingly using the ECMWF analysis and forecast wind fields. The aim of the study is to evaluate the effect of the ERS-1 data computing the statistics of the analysis and of the forecast up to the 5 days range.

The paper is organized in the following way. The whole assimilation procedure is described in section 2 considering separately its three main components: the analysis of the SWH (Section 2.1), the analysis of the wind field (Section 2.2) and the analysis of the spectrum (Section 2.3). The organization of the assimilation experiment and some general aspects of the wave fields are described in Section 3. Section 4 shows the effect of the assimilation on the wave analysis and section 5 shows the effect of the assimilation on the wave forecast. The main outcomes of the study and some possible developments of this assimilation scheme are discussed in Section 6.

[1] "Data assimilation in Marine Science", Liege, May, 1993.

2. The data assimilation scheme

The dynamical quantity whose evolution is computed by the WAM model is the wave spectrum. The goal of the assimilation is therefore to produce analysed spectra. The altimeter does not provide with a complete information, because the structure of the wave spectrum, the mean frequency, and the mean direction are left undetermined. Only the SWH is measured. This sequential scheme compensates for the missing information with a procedure that is split into two steps. In the first one (described in Section 2.1 the analysed SWH field is built using O.I. (Optimal Interpolation). In the second one (described in Sections 2.2 and 2.3) the analysed SWH field and and the first guess spectra are used to construct the analysed spectra and to evaluate the analysed friction velocity.

The assimilation procedure consists of a series of N independent corrections, each at a different time t_i, $(i = 1, \dots N)$, and each using the altimeter SWH data available in a time window centered at the time t_i. At each time t_i the wave field is modified, taking into account the reliability of both model results and measurements [2]. In the present implementation $t_i = t_{i-1} + \Delta t$, where the interval Δt is six hours, which is also the width of the time window used.

2.1. The analysis of the swh field

At the assimilation times t_i the first part of the procedure computes an analysed SWH field by O.I.

At each point x_i the analysed SWH H_A^i is expressed as a linear combination of the first

[2] No interpolation in time was carried out in order to compensate the difference between t_i and the time of the observations.

guess predicted by the model H_P^j, and of the observations H_O^j

$$H_A^i = H_P^i + \sigma_P^i \sum_{j=1}^{N_{Obs}} W_{ij} \frac{H_O^j - H_P^j}{\sigma_P^j}, \tag{2}$$

where N_{Obs} is the number of available observations and σ_P^j is the root mean square error in the model prediction:

$$\sigma_P^i = \left\langle \left(H_P^i - H_T^i\right)^2 \right\rangle^{1/2} \tag{3}$$

Here H_T^j represents the true value of SWH. The subscripts A, T, and P denote respectively the analysis, the truth and the prediction. The weights W_{ij} are chosen to minimize σ_i^A, the root mean square error in the analysis,

$$\sigma_A^i = \left\langle \left(H_A^i - H_T^i\right)^2 \right\rangle^{1/2} \tag{4}$$

and they are given as

$$W_{ij} = \sum_{k=1}^{N_{obs}} P_{ik} M_{kj}^{-1}, \tag{5}$$

where the element of the matrix **M** is

$$M_{kj} = P_{kj} + O_{kj} \tag{6}$$

and P and O are the error correlation matrix of prediction and observation respectively. The $\langle \rangle$ indicates the average over a large number of realizations. The correlation matrices needed to compute the weights W_{ij} are specified as it follows:

$$P_{kj} = \left\langle \frac{\left(H_P^k - H_T^k\right)\left(H_P^j - H_T^j\right)}{\sigma_P^k \sigma_P^j} \right\rangle = \exp\left(- \frac{|\bar{x}_k - \bar{x}_j|}{L_{max}} \right), \tag{7}$$

$$O_{kj} = \left\langle \frac{\left(H_O^k - H_T^k\right)\left(H_O^j - H_T^j\right)}{\sigma_O^k \sigma_O^j} \right\rangle = \delta_{ij} \frac{\sigma_O^i}{\sigma_P^i}. \tag{8}$$

in the set-up used $\sigma_O^i = \sigma_P^i$ and L_{max} is equal to five grid steps. In principle the parameters could be modified, by varying them in both space and time. The a-priori estimation of P and O is a weak point of the assimilation experiment. In a preliminary assimilation experiment (Lionello et al., 1992), it was found that the values used maximized the benefits of the assimilation.

2.2. The analysis of the wind field

In absence of boundaries (i.e. with an infinite fetch) the energy of the windsea is determined by the wind speed U_{10} — or alternatively by the friction velocity u_* — and by the duration t. One has $E = E(t, U_{10})$ or $E = E(t, u_*)$. Using scaling arguments (Kitaigorodskii, 1962) one can write $E_* = E_*(t_*)$, where

$$E_* = \frac{g^2}{u_*^4} E, \; t_* = \frac{g}{u_*} t. \tag{9}$$

From the WAM model growth curve one derives

$$E_*(t_*) = 955 \tanh(6.02 \cdot 10^{-5} t_*^{0.695}). \tag{10}$$

Eqs. (9) and (10) are used twice. First the friction velocity and the energy are substituted with their first guess value, $u_* = u_{*P}$ and $E = E_{Pws}$, and the equations give the duration t_P of the windsea. Successively the windsea energy is substituted with its analysed value, $E = E_{Aws}$, the first guess duration is assumed to be correct, $t_A = t_P$, and the equations give the analysed friction velocity u_{*A}. The wind speed is subsequently derived using the model drag coefficient.

The first guess windsea energy E_{Pws} is estimated searching for a peak within an angle of 30° from the wind direction. If a peak with a frequency larger than the Pierson– Moskowitz frequency is found then the energy of the windsea is evaluated using Eq. (10) (see Lionello et al., 1991). The analysed windsea energy is computed assuming that the ratio between the windsea and the total energy was predicted correctly:

$$E_{Aws} = E_{Pws} \frac{H_A^2}{H_P^2}. \tag{11}$$

Eq. (10) is a simple tool to derive the analysed wind speed from the analysed SWH value in the presence of windsea. Of course the estimate is incorrect in the vicinity of the coast when the wind is blowing offshore and the energy of the wave is a function of the fetch. This effect would be definitely important in a high resolution regional implementation of the WAM model. In a global application this shortcoming does not prevent a reasonable estimate of the wind speed in most of the interesting cases.

The estimate is provided only in the presence of windsea. The analysed friction velocity cannot be derived from the swell spectrum because it is not related to the local wind. In this case the first guess value is not changed by the assimilation scheme.

In the absence of any feedback to the atmospheric circulation model producing the wind fields only the current wind field is modified by the assimilation scheme and the model is driven by the analysed friction velocity until a new wind field is used.

2.3. The analysis of the wave spectrum

This part of the procedure reconstructs the spectrum from the analysed SWH. It transforms the first guess spectrum into the analysed one, using the total energy as the only information. The first guess spectrum $F_P(f, \theta)$ is used to produce an analysed spectrum $F_A(f, \theta)$ as

$$F_A(f, \theta) = AF_P(Bf, \theta). \tag{12}$$

The energy of the spectrum is scaled by the factor A to modify the SWH, and the frequency scale is stretched (or contracted) to modify the peak frequency. No information is available on the mean direction and the directional distribution is consequently not modified.

The determination of the two parameters A and B in Eq. (12) is the purpose of this second part of the procedure. It depends on the type of process undergone (Lionello et al., 1992). The procedure distinguishes between windsea and swell.

– Windsea

The reconstruction of the windsea spectrum is obtained using its growth curve given by (Eq. 10) to compute its duration and the friction velocity according to the procedure that has been explained in Section 2.2. The analysed mean frequency f_{mA} is derived from the analysed energy and friction velocity using the relations

$$f_{m*} = \frac{u_*}{g} f_m, \tag{13}$$

$$E_* = 1.68 \cdot 10^{-4} f_{m*}^{-3.27}. \tag{14}$$

Eq. (14) is a fit to the WAM model curve for a time limited growth. The two quantities A and B are given as:

$$A = \frac{E_A}{E_P} B, \; B = \frac{f_{mP}}{f_{mA}}, \tag{15}$$

– Swell

The swell spectrum is modified according to the method proposed by Lionello and Janssen (1990), i.e. without modifying its average steepness. This gives:

$$A = \frac{E_A}{E_P} B, \; B = \Delta \left(\frac{E_A}{E_P} \right)^{1/4}, \tag{16}$$

where Δ is a factor very close to one. The rescaling of the frequencies is necessary in order to produce an analysed spectrum corresponding to waves of sensible steepness. In particular the enhancement of the spectral level without moving the peak toward lower frequencies, would produce a very high dissipation that would greatly diminish the effect of the assimilation (Lionello and Janssen, 1990).

If swell and windsea are simultaneously present the parameters A and B are computed according to the dominant part of the spectrum. This reflects the limitation of this method that is not able of modifying the ratio between the windsea and the swell

If the duration t_A is wrong the analysis of both the friction velocity and the windsea is incorrect. In fact the underestimate of t_A implies the overestimate of u_{*A} and consequently of f_{mA}.

3. A one month operational assimilation experiment

The global wave prediction was carried out in February 1992 at the ECMWF, using the wind fields produced by the atmospheric circulation

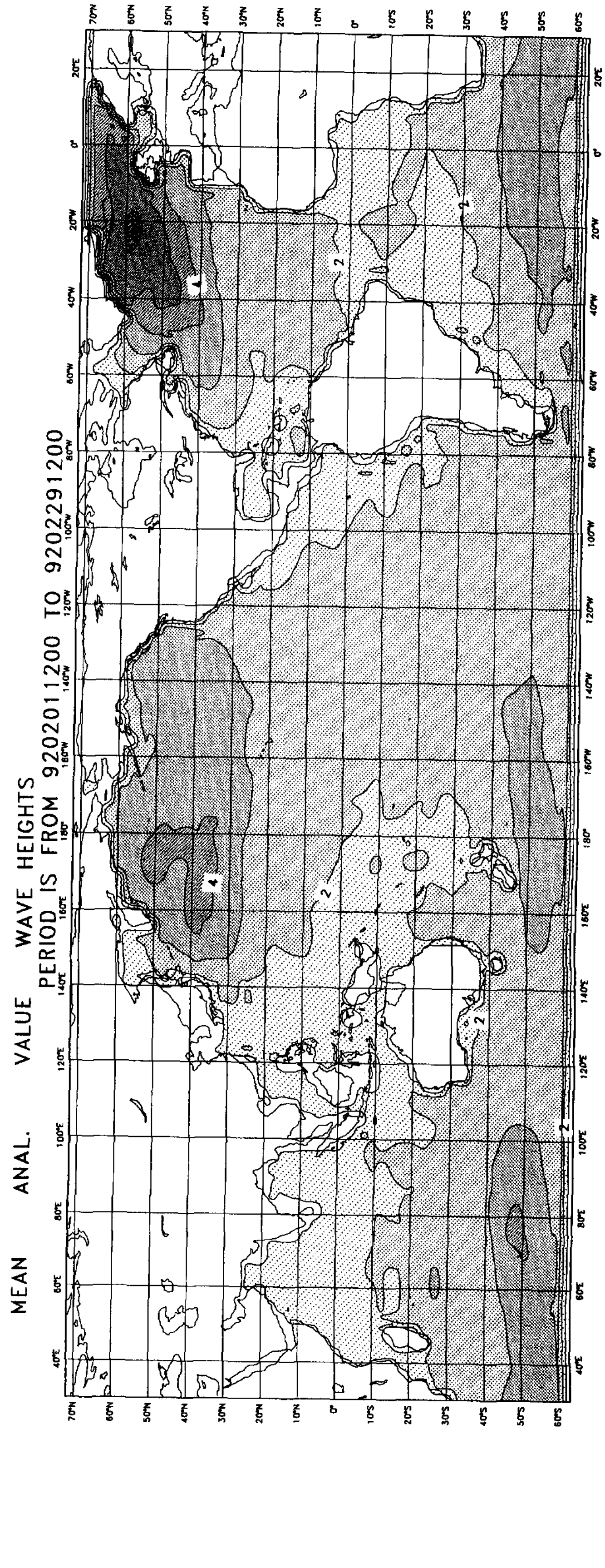

Fig. 1. Average analysed SWH computed assimilating the ERS-1 altimeter data during the whole month of February 1992. The isolines are drawn every 1.0 m.

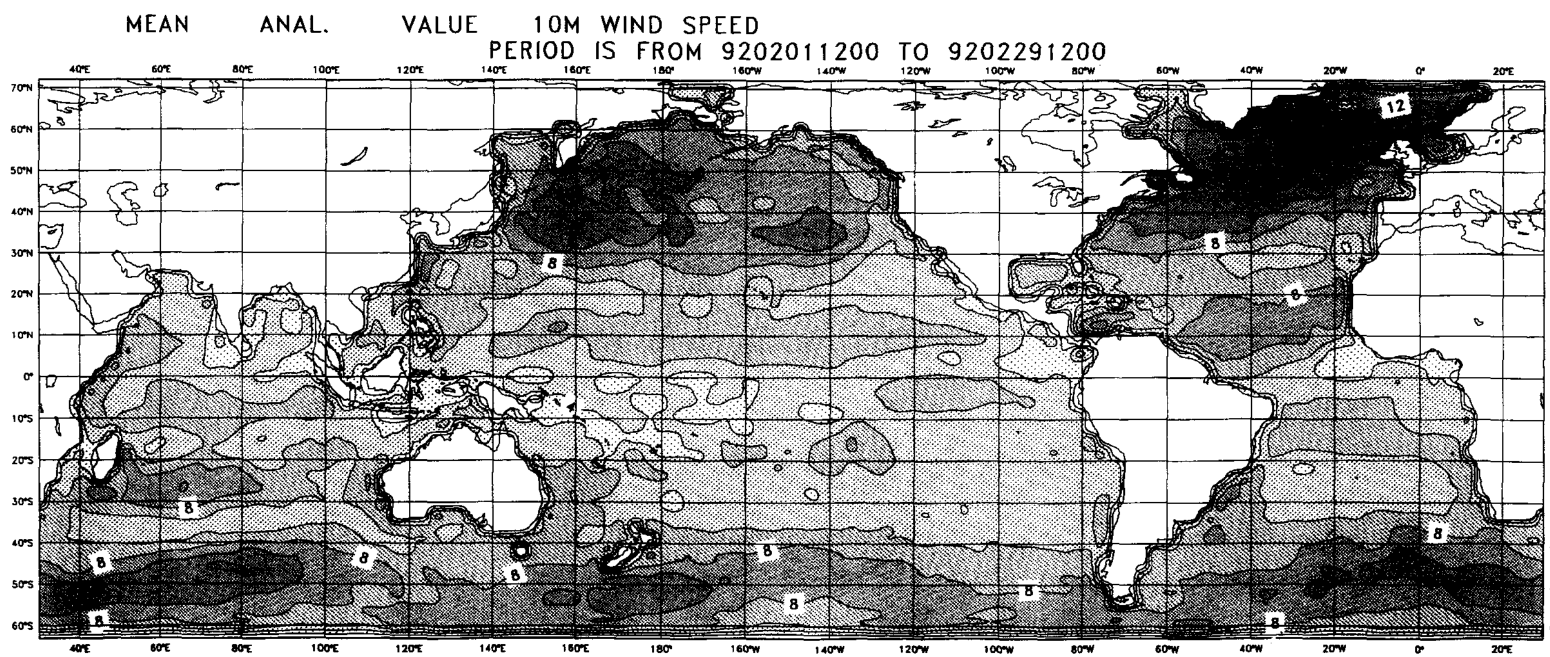

Fig. 2. Average analysed 10 m wind speed computed assimilating the ERS-1 altimeter data during the whole month of February 1992. The isolines are drawn every 2.0 m.

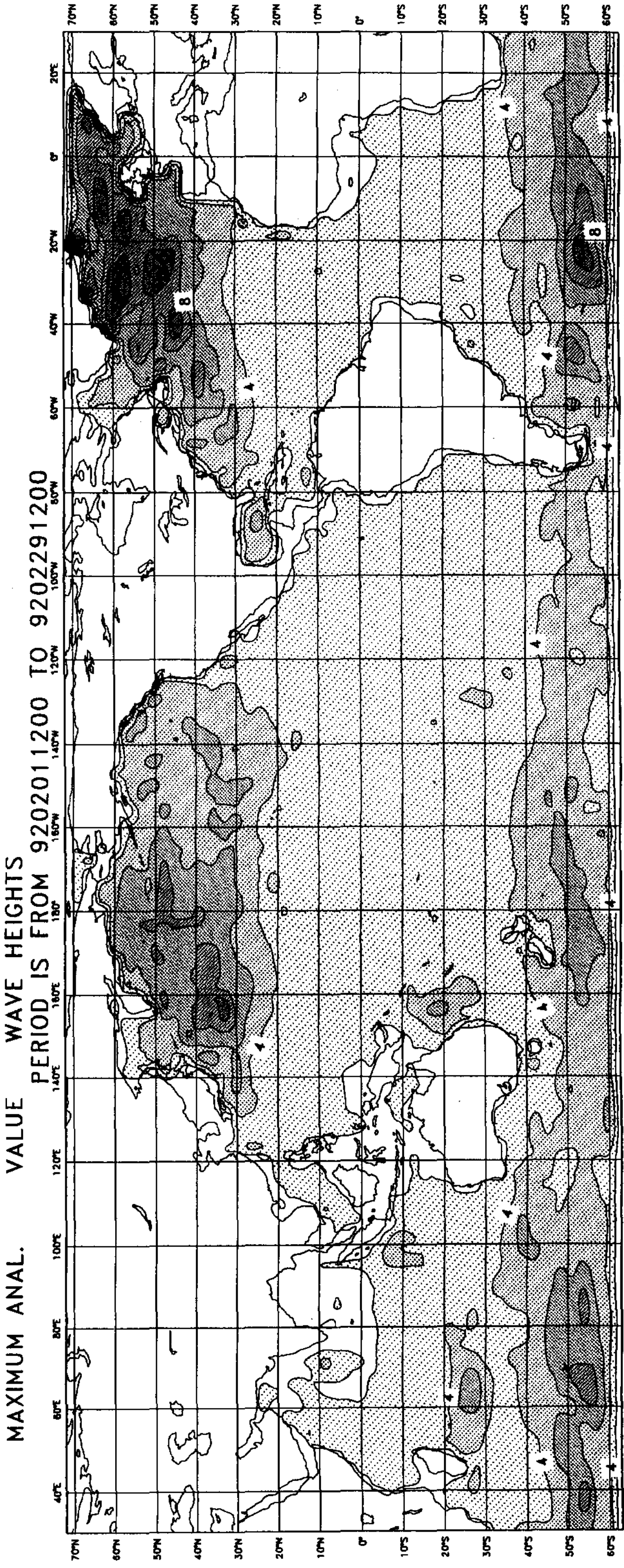

Fig. 3. Maximum analysed SWH computed assimilating the ERS-1 altimeter data during the whole month of February 1992. The isolines are drawn every 2.0 m.

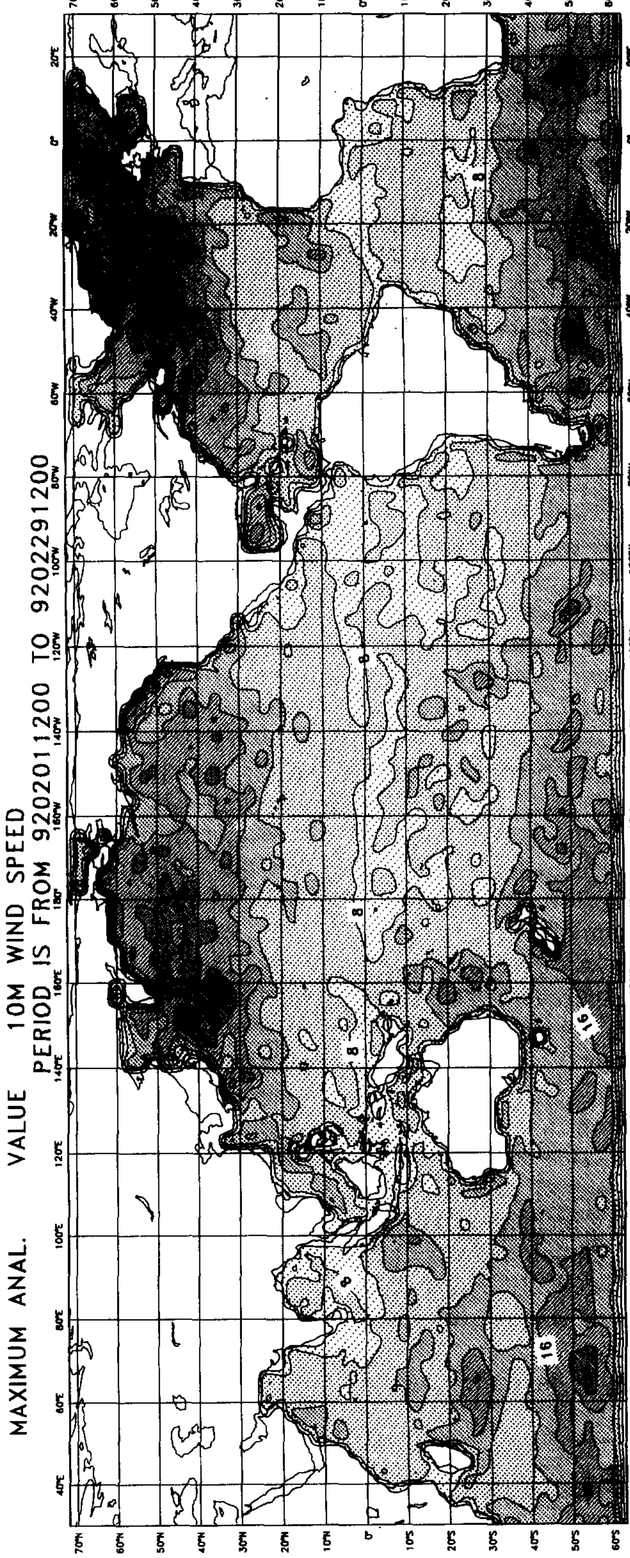

Fig. 4. Maximum analysed 10 m wind speed computed assimilating the ERS-1 altimeter data during the whole month of February 1992. The isolines are drawn every 4.0 m.

model of the centre. The assimilation was performed in an operational mode and in quasi real time, using the ERS-1 data available during the whole month.

Two experiments have been carried out in parallel: an assimilation experiment using ERS-1 altimeter data and a reference experiment without assimilation. Each experiment consists of a series of 29 runs, one every day. Each run is split into an analysis period, whose length is one day, and a forecast period, whose length is five days. The initial wave field of each run was the wave field of the previous run at the end of the analysis period. In both experiments the model was driven by the ECMWF analysed wind fields during the analysis period and by the ECMWF forecast wind fields during the forecast period. A new wind field was fetched every six hours, keeping it constant for a six hours time window. In the assimilation experiment the ERS-1 SWH measurements were assimilated during the analysis period, while no wave data has been used in the reference experiment. The assimilation was carried out every six hours, at the central time of the wind time window.

The global application for the whole month of February gives the opportunity to apply the data assimilation to all sorts of wave conditions. Fig. 1 shows the spatial distribution of the average [3] analysed SWH and Fig. 2 the average analysed 10 m wind in the assimilation experiment. The high values in the northern latitudes are associated with the occurrence of intense winter storms. There are many storms also in southern latitudes, but they are less intense during this part of the year, and the average SWH value is lower. The tropical oceans are mostly covered with systems of relatively low waves. Most of them are swell. In fact the average SWH distribution reflects the pattern of the average wind speed in the high and low latitudes, while it is independent of wind speed variations in the tropics.

The following Figs. 3 and 4 show the spatial distribution of the SWH maxima [4] and wind speed maxima respectively. Like in the previous figures the highest values are located in the northern and southern latitudes. One can see that in these two areas the pattern of the SWH maxima closely resembles the pattern of the wind speed maxima, while in the tropics there is no relation between the flat SWH maxima distribution and the wind speed distribution. This is because the maxima in the SWH are due to the highest wind speeds along the storm tracks. Therefore in the northern and southern part of the globe the highest wave conditions are due to the local wind. In the tropics the highest waves were in many cases generated by distant storms and they travelled with hardly any dissipation after they left the storm area, covering a long distance, but changing little in their SWH values. This explains the flat distribution in the tropics.

In the northern regions of the globe and in the vicinity of the eastern coast of the oceans one notices that the peaks of the maximum SWH tend to move eastwards with respect to the peaks of the maximum wind speed. The reason is the prevalent eastward direction of the winds and consequently the eastward increasing fetch. In fact the waves can continue growing under the action of the wind after the actual maximum wind speed has been left behind.

Differences between the impacts of data assimilation on the different wave regimes are expected. A uniform swell system, travelling for a long time over the ocean without large changes in its intensity is more likely to be detected by the satellite than an intense windsea lasting for the duration of the storm and confined to the area of the storm. Moreover, the assimilation of a swell system has a longer lasting effect than the assimilation of windsea. Since the energy dissipation is very small for a swell, the swell will keep the memory of the assimilation until it reaches the coast or it is modified by a storm along its path. A windsea, that is continuously evolving under the

[3] The average value is computed separately for each grid point using the values output every six hours by the model during the whole month.

[4] The maxima are computed separately for each grid point. They represent the maximum value reached locally during February.

MEAN (ASSIM - REF) WAVE HEIGHTS IN FEBRUARY 1992

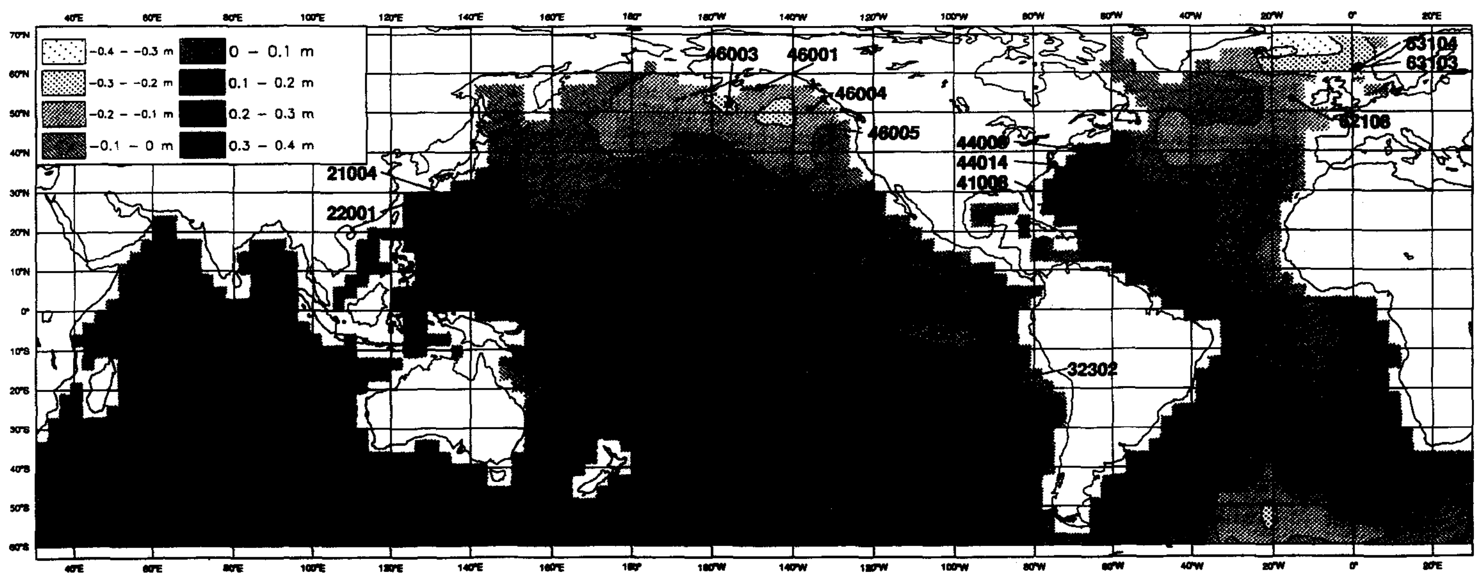

Fig. 5. SWH bias between Ra and Aa: $\langle H_A - H_R \rangle$ where H_A is the value produced by Aa and H_R is the value produced by Ra. Here $\langle\rangle$ denotes the monthly average in each model grid point. Darker areas denotes positive values, ligher areas negative values. The figure shows the positions of the buoys considered in this study.

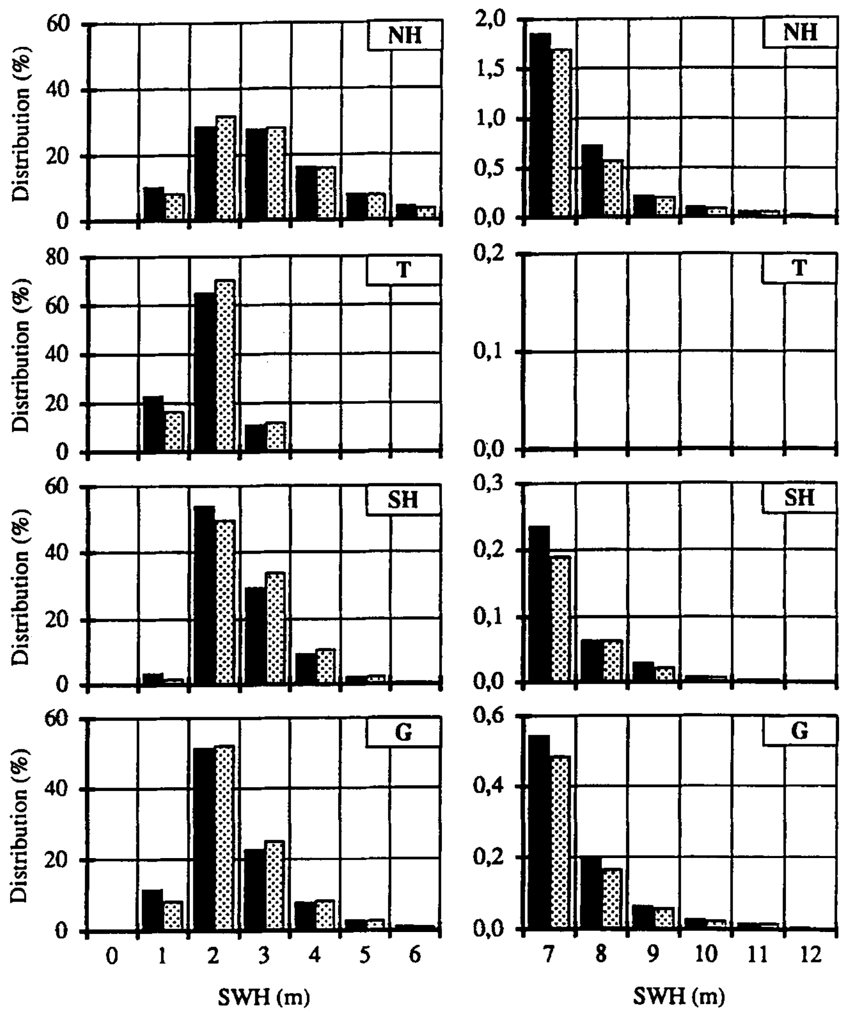

Fig. 6. SWH distribution for the run Ra (full bars) and Aa (dotted bars). From top to bottom: northern part (*NH*), tropics (*T*), southern part (*SH*) and global (*G*) distributions. Left panels: SWH from 0 to 6 m. Right panels from 7 to 12 m.

influence of the wind, begins losing the memory of the assimilation as soon as the analysed wind field is removed. Therefore to assimilate consistently the wind speed and the SWH is essential for an efficient windsea assimilation. In the present model set-up, where only the current wind field is modified, no long lasting effect can be expected from the wind sea assimilation [5].

[5] The analysed wind is used only for the rest of the time window, i.e. for three hours after the assimilation.

4. The analysis of the global wave field

In this study the term analysis refers to the first part of each model run during which the wave field that represents most accurately the true one is constructed. In the reference experiment this goal is pursued by driving the WAM model with the analysed ECMWF wind fields. In addition during the assimilation experiment the model results are combined with the ERS-1 altimeter observations, i.e. the wave data are assimilated. To have a good analysis is the requisite for the production of a good forecast, and to improve the quality of the wave analysis is the purpose of the assimilation procedure.

The first point to investigate is the size of the effect of the assimilation. Two different analysed fields are computed daily every six hours. One has been computed in the reference experiment (denoted as Ra) and another in the assimilation experiment (denoted as Aa). Note that while Aa is truly an analysed wave field, where model first guess and measurements have been combined to obtain the best estimate, Ra is an analysed field only because it has been produced using analysed wind fields.

Fig. 5 shows the distribution of the bias

$$Bi = \langle H_{Aa} - H_{Ra} \rangle = \frac{1}{N} \sum H_{Aa}(i) - H_{Ra}(i) \quad (17)$$

over the model grid (the average is computed over the whole month of February for each grid point). The bias is in the range between −30 and +30 cm. It is small and positive in the tropics; large and negative in the northern Pacific and northern Atlantic; negative in the Atlantic sector of the southern ocean; and positive in the Pacific sector of the southern ocean.

Some more insight is obtained by observing the modifications of the SWH distribution produced by the assimilation (Fig. 6). The number of high sea states and of very low sea states is reduced. The overall effect of the assimilation is to concentrate the waves in an intermediate range, say between 2 and 7 m. In order to examine the differences of the impact in the various parts of the globe the statistics have been separately computed for three different regions: tropical region (between 20°N and 20°S), southern region (latitude lower than 20°S) and northern region (lati-

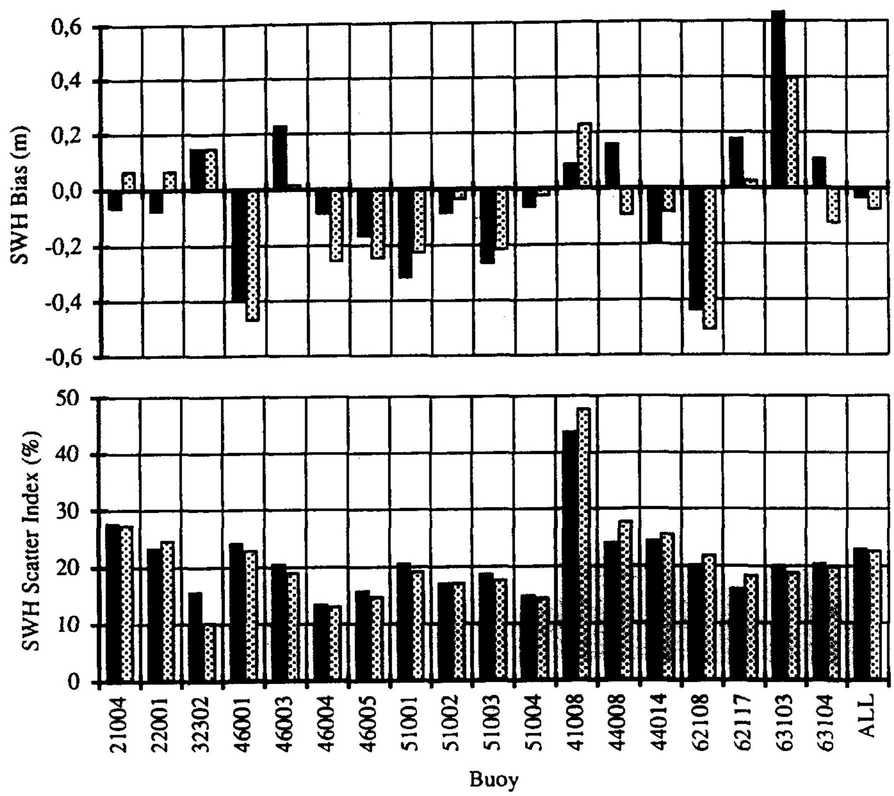

Fig. 7. Buoy statistics. The full bars refers to the reference (Ra) and the dotted bars refer to the assimilation (Aa). The upper panel shows the bias (model–buoy) and the lower panel the scatter index.

tude larger than 20°N). The attenuation of the high waves is the dominant effect in the northern area. The inspection of single events shows that the negative bias is associated with the reduction of the waves at the peak of the storms. In the tropics there is a relevant amount of low sea states that have been increased. This is associated with a small increase of the low swell, which is modified over very large areas of the ocean. The southern area is similar to the northern area, but the ice boundary was poorly reproduced in the wave model, and the absence of seasonal variation, that strongly affects the fetch, is a possible source of error, whose importance was not controlled.

Fig. 5 shows the buoys that are available for validation on a global scale. Fig. 7 shows the bias of the model SWH H_M against the buoy SWH H_B,

$$Bi_b = \frac{1}{N} \sum H_M(i) - H_B(i) \tag{18}$$

and the Scatter Index

$$SI = 100 \frac{\left[\frac{1}{N-1} \sum \left(H_M(i) - H_B(i) - Bi_b \right)^2 \right]^{1/2}}{\frac{1}{N} \sum H_B(i)} \tag{19}$$

In most cases the SI is lower for the assimilation than for the reference. Since the overall SI denoted with "ALL" has been reduced by the assimilation — even if the reduction is small — we conclude that it improved the results of the model, although the effects of the assimilation are not homogeneous. Results are particularly good in the tropics, i.e. for the buoy 32302, located near Peru's coast and the buoys 51001, 510002, 51003, 51004 at Hawaii. Impact on the scatter index is positive in most of the cases for buoys 46001,46003, 46004 and 46005 in the Gulf of Alaska although, consistently with the previ-

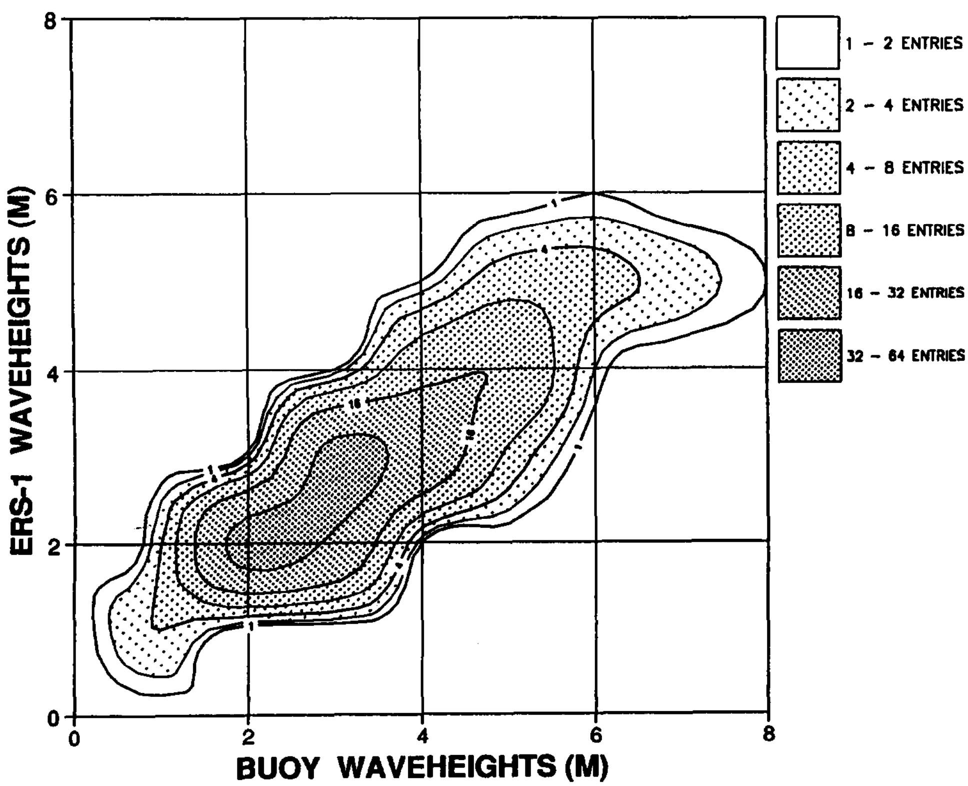

Fig. 8. Scatter diagram, ERS-1 altimeter against buoy measurements in February and March 1992.

ously discussed reduction of high wave conditions, the negative bias of the model is further increased in magnitude. The effect of the assimilation is negative for buoys 21004 and 22001, located in the western Pacific, south of Japan, and for the buoys 44008, 44014, 41008 in the western Atlantic, close to the U.S. coast. Results are instead positive for buoys 63104 and 63103 in the Norwegian Sea, while they are negative for the buoy 62108 in the northeastern Atlantic.

The buoys can be divided into three classes. The first class includes the buoys that are located near the west coast of the oceans and which are only slightly affected by the assimilation of the satellite data, generally because the waves are rarely detected by the altimeter before reaching the buoy location. The second class includes the buoys that are located in the tropics, where the SWH has moderate values and the impact of ERS-1 data is positive. The third class includes the buoys located in the northeastern part of the oceans, where the SWH has generally large values and the impact of ERS-1 data is not always good. Unfortunately no buoys are available in the southern Ocean.

We conclude that the comparison between Aa and Ra runs against the buoy data shows that the assimilation improves the agreement between model analysis and buoy data, although there are cases, generally in the presence of extremely high SWH events and for local conditions where the agreement deteriorates. Since we believe that buoy measurements are precise, it implies that the assimilation has not always improved the model results.

In our opinion the explanation is that the altimeter is low with respect to the buoys for high SWH values. This is evident in the fig. 6 of Goodberlet et al. (1992), where buoy data and ERS-1 altimeter data are compared. It is also

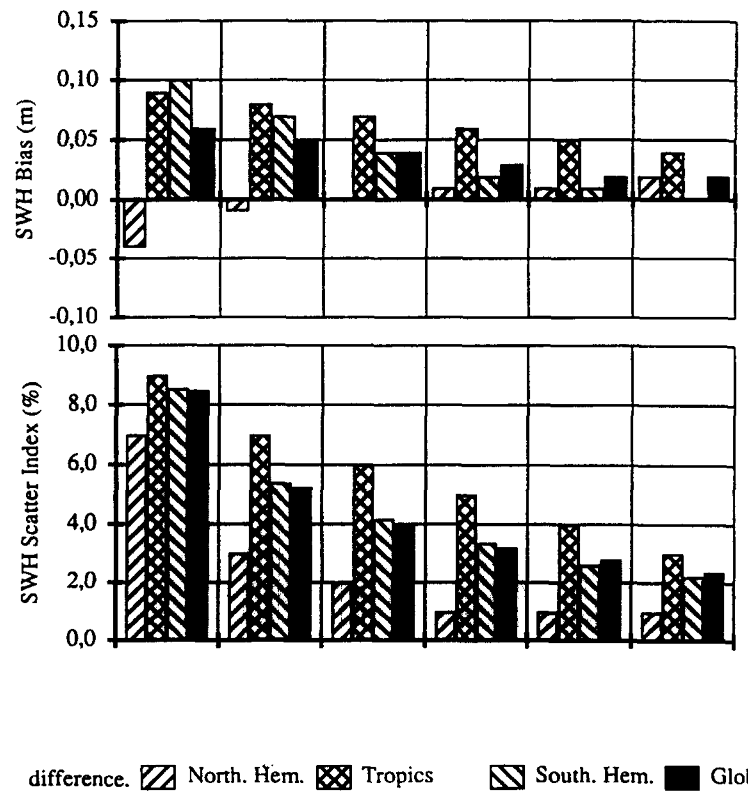

Fig. 9. Statististics of the reference experiment against the assimilation experiment. Top: bias (Assimilation–Reference), Bottom: scatter index.

evident in the data that we used here. Fig. 8 shows the scatter diagram of buoys against the ERS-1 altimeter for the month of February and March 1993. The satellite data within a distance of 160 km of the buoy location and contained in a six hours time window centered at the time of the buoy measurements have been collected and their average value plotted against the buoy measurement. The distribution shows a reasonable agreement between the two data sources. The overall bias (0.23 m) indicates that the ERS-1 altimeter is on the average lower than the buoys. A more accurate analysis of the distribution shows actually that for waves higher than 6 m the agreement is poor and buoy measurements over 6 m correspond to ERS-1 measurements below 6 m. This means that if only high waves are considered the altimeter is lower than the buoys. We think that this discrepancy explains why the improvement produced by the ERS-1 data on the agreement between model and buoys for peak events is not satisfactory.

The magnitude of discrepancies between model and buoys offer a scale to judge whether the effect of the assimilation is "important". In this sense it is erroneous to dismiss a change of a few centimeters in the bias as "small" in the tropics. In fact the comparison against the buoy time series indicates that its magnitude is actually close to the bias between the model and the buoy. Moreover when the average impact of the ERS-1 data on the model time series is of a few centimeters, the single values are modified by a few tens of centimeters, compensating a relevant part of the difference with the buoy data (more details are presented in Günther et al., 1993). This is to say that in many cases the corrections are of the order of the model inaccuracies in the tropics. Unfortunately, with respect to the discrepancies between model and buoy at more northern latitudes the corrections are small and not satisfactory.

5. The forecast of the global wave field

In the previous section we discussed the impact on the wave analysis. In this section we discuss how much this impact persists after the end of the analysis and how far into the forecast range the eventual benefits of ERS-1 data can be identified.

The persistency can be evaluated from Fig. 9, where assimilation and reference experiments are compared computing bias and scatter index between the two experiments as a function of the forecast range. The initial fields of the forecast, i.e. the final fields of the analysis periods Ra and Aa, are different, because of the data that have been assimilated in Aa, but the reference and the assimilation experiments use the same wind fields during the forecast period. Fig. 9 shows the progressive decrease of the initial difference between the two experiments by the action of the wind. The magnitude of the bias becomes smaller as the forecast range extends. Its rate of decrease shows large regional variations. The effect of the assimilation is much more persistent in the tropics, where there are mostly swell systems with a very long decay time scale. This is because around the Equator the wind is low, and its action on the waves, mostly originated in the northern and southern latitudes, is generally weak. Examining the decay of the magnitude of the bias one can guess a linear decay in the tropics (due to the advection of the wave energy out of the basins), and an exponential decay in the two other areas (due to the action of the wind). The scatter behaves in an analogous way.

As the forecast range extends the errors in the model results grow larger and the computed wave field becomes increasingly different from the real one. The best knowledge that we have of the real waves in the ocean is given by the model analysis in the assimilation experiment, where measurements and model results have been merged to produce the best representation of reality. The agreement between the forecast and Aa is therefore a measure of the quality of the forecast. This is quantified by the forecast skill

$$SK = 1 - \sum \left[H_{Aa}(i) - H_F(i) \right]^2 / \sigma_C^2, \tag{20}$$

where H_{Aa} is the analysed SWH, H_F is the corresponding forecast value, and σ_C^2 is the climatological variance. Fig. 10 shows the skill as a function of the forecast range for both reference and assimilation experiment. The skill is higher, both globally and in each area, for the assimilation than for the reference experiment, indicating the positive effect of the ERS-1 data on the wave forecast. The improvement is large in the tropics, where it persists for a long time and it is still present in the five day forecast. It is small in the northern part, where it is hardly visible in the two days forecast.

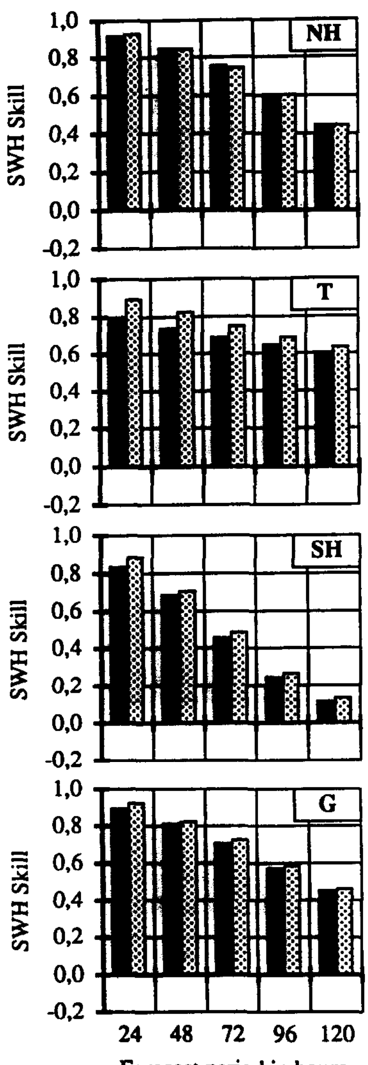

Fig. 10. Forecast skill. Full bars denote the reference experiment and dotted bars denote the assimilation experiment. All bars are normalized by the variance in the analysis of the assimilation experiment Aa. From top to bottom: northern part (*NH*), tropics (*T*), southern part (*SH*) and global (*G*).

The comparison against the buoys is conditioned by the disagreement between the ERS-1 data and the buoy data, already discussed in section analysis. The statistics are computed separately for the analysis (denoted with "A") and for the forecasts (denoted with the respective range in hours), and by grouping the buoys regionally. Fig. 11 shows that the impact on the bias persist in time, but the reduction of the scatter does not persists longer than one day. There is a positive impact at Hawaii — see the panels denoted with "HAW" — and in the southeastern Pacific — see the panels denoted with "SEP" —, but there is a little impact in the remaining regions. In the southeastern Pacific, namely buoy 32302, the benefits in the reduction of the scatter are clear even after 5 days. This is clearly related to the massive presence of swell during the summer season. For Hawaii, where one could expect a similar situation, the intense storms, relatively near and sometimes hitting Hawaii itself, prevent an analogous persistency. In the other parts of the globe one observes a rapid loss of the ERS-1 effect caused by the continuous action of the wind.

The ERS-1 data are not used during the forecast. Therefore they are an independent dataset, and both the assimilation and the reference experiments can be validated against them. The comparison was carried out computing the model equivalent of the altimeter data, i.e. the model results were interpolated in space and time to the time and the position of the satellite measurements. Results are shown in Fig. 12. The bias and the scatter index are smaller in the assimilation run than in the reference both regionally and globally (there are some exceptions like the 96 and 120 hours forecast for the northern area). The impact of the assimilation is persistent and the assimilation run produces results more in agreement with the ERS-1 altimeter than the reference run.

The use of the buoy data and of the altimeter data for the validation of the results suggests different conclusions. If the discrepancies be-

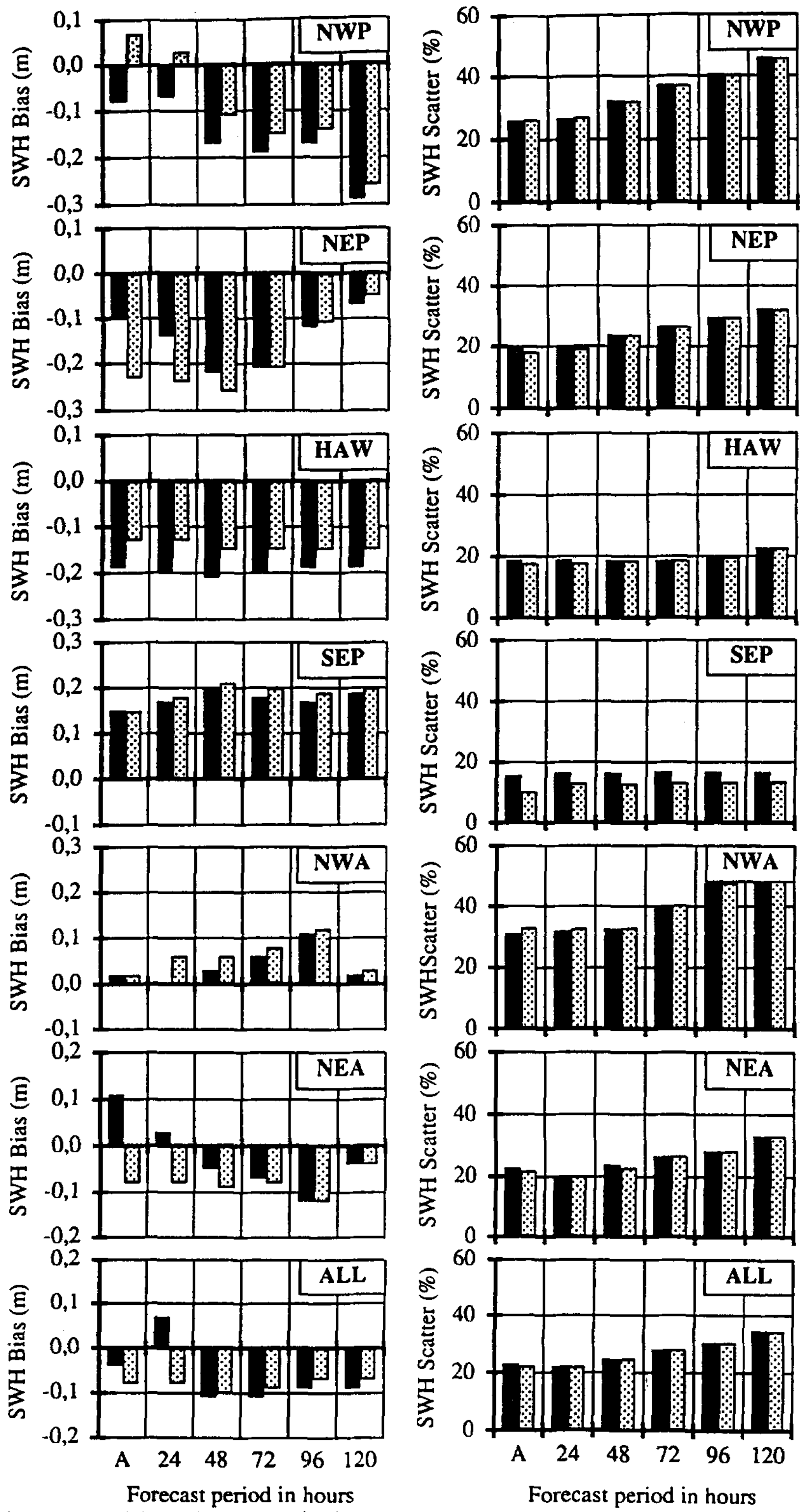

Fig. 11. Comparison between model and buoy. Bias (left) and Scatter Index (right) for the analysis and for the various forecast ranges. The buoys are grouped in regions. From top to bottom: Northwestern Pacific (*NWP*), Northeastern Pacific (*NEP*), Hawaii (HAW), Southeastern Pacific (*SEP*), Northwestern Atlantic (*NWA*), Northeastern Atlantic (*NEA*) and global (*ALL*). Full bars denote the reference and dotted bars denote the assimilation.

tween buoy data and the model are considered, then the effect of the assimilation is not impressive, and it is convincing only in the tropics. On the other hand, if the discrepancies between the altimeter and the model are considered, then the effect is evident and positive, because a substantial reduction of the differences between model and measurements has been obtained. We think that this shows that the assimilation method works properly and the differences between the assimi-

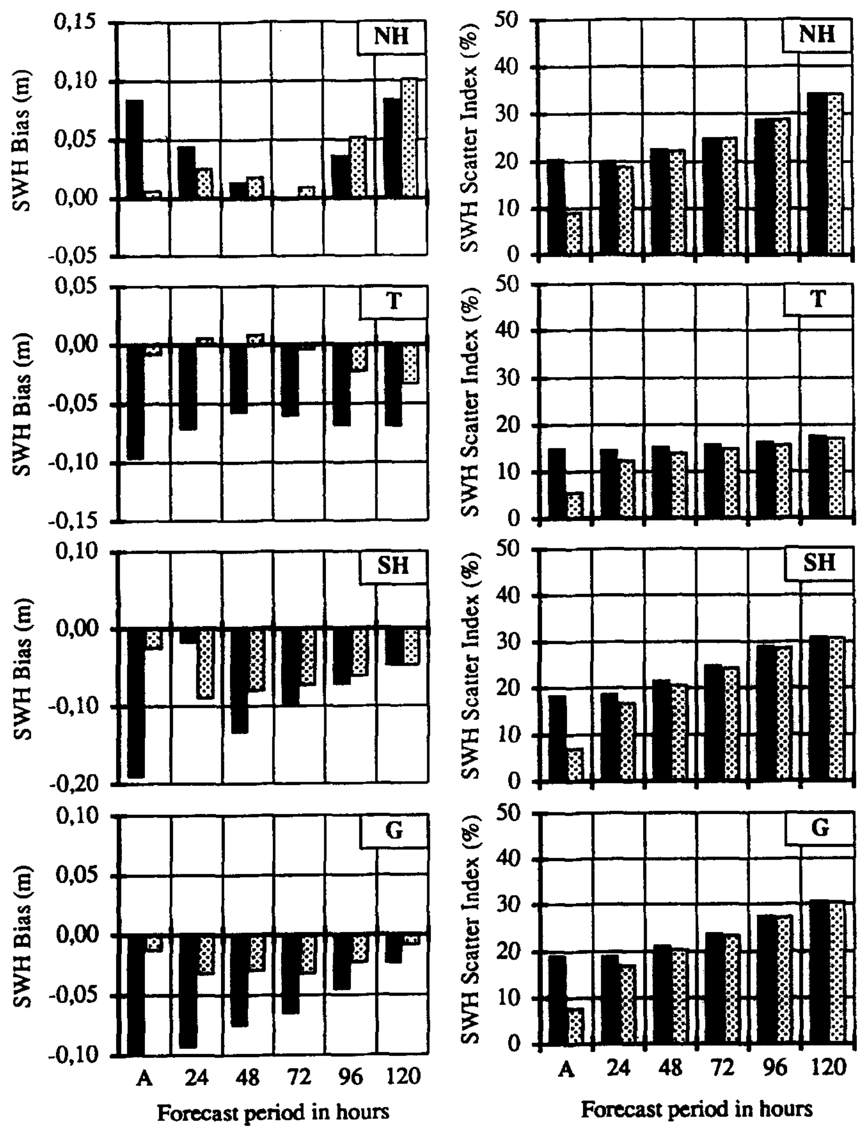

Fig. 12. Comparison between model and altimeter. The panels show the bias (left) and the Scatter Index (right) for the analysis (A) and the various forecast ranges. Full bars denote the reference experiment and dotted bars the assimilation experiment. From top to bottom: northern part (*NH*), tropics (*T*), southern part (*SH*) and global (*G*).

lated data and the buoys are the source of the unsatisfactory results.

6. Conclusions

The comparison of assimilation results and buoy measurements is only in part satisfactory. The wave analysis and the scatter diagram of colocated buoy and altimeter data show that the ERS-1 altimeter measurements are low for high waves and high for low waves with respect to the buoys. The data are little affected by this disagreement in the tropics, where the SWH has moderate values, but the difference is important in the northern Atlantic and in the northern Pacific, where the SWH reaches extreme values.

In the tropics, the variations produced on the average analysed SWH by the assimilation are not much smaller than the bias between the model and the buoys, i.e. they compensate a substantial fraction of the difference between the model and the buoys. For the buoys located in other regions, i.e. in the Gulf of Alaska and in the northern Atlantic, the variations have the same magnitude, but they have a minor importance because the discrepancies between the model and the buoys are much larger.

The same conclusion is valid for the forecast. The effect of the assimilation on the forecast is small with respect to the difference between the reference experiment and the buoys, which is compensated in little part. Only the buoys in the tropics, which in the statistics are denoted as "SEP" and "HAW", indicate a persistent and favourable impact of the ERS-1 data. In spite of this partially unsatisfactory situation, there are other indications showing that the assimilation has a positive effect.

In fact, first of all, the comparison between model forecast and altimeter shows the persistency of the benefits achieved during the analysis. The assimilation experiment improves with respect to the reference experiment, especially in the tropical area, where the reduction in the magnitude of the bias is still present in the five day forecast. Also the reduction of the scatter index, though less persistent, is significant. Moreover, the comparison between the wave forecast and the wave analysis shows that ERS-1 data have a positive impact on the prediction skill. They improve the quality of the wave forecast, increasing its similarity with the analysis.

Finally, the comparison between the assimilation and the reference experiment shows the decay rate of the the effect of the assimilation. The global decay time is about three days, but there are differences in the various parts of the globe, according to the dominant wave regime. In the northern and southern latitudes, where wind is active, the decay time is between two and three days, while in tropical regions it is about five days.

The performance of this sequential assimilation approach can be improved. In particular, the error correlation matrices of both the model and the observations can be evaluated more accurately, and the assimilation can account for their variations according to the characteristics of the wave spectrum and the meteorological situations (e.g. different correlation lengths could be used for the windsea and for the swell). On the other hand there are shortcomings that cannot be avoided while dealing with the altimeter data. It appears difficult to establish general criteria for changing the mean direction of the waves, for changing the ratio between the windsea and the swell, for recovering a peak that is absent, and generally for reorganizing the structure of a spectrum that was basically incorrect in the first guess. In our opinion these problems can be avoided using more complete information, i.e. by extending this scheme to assimilate SAR spectra (Hasselmann et al., 1993).

We think that it is still an open question if it is more convenient to follow a sequential or a variational approach in the practical use of the available satellite data, although, the variational approaches have the advantage of accounting naturally for the model dynamics. Anyway we think that the SAR data should be used without necessarily waiting for a variational approach to be ready and we expect to get interesting new material for discussions from the forthcoming attempts to assimilate the SAR spectra provided by the ERS-1 using OI. Considering the present state-of-the-art the sequential approaches in any case get the credit for the first successful realistic experiments. They allowed us to use the data provided by the satellites and to intercompare measurements, thus learning about their reliability.

Acknowledgements

The work carried out by P. Lionello at the Max-Planck-Institute für-Meteorologie was supported by ESA.

References

Esteva, D.C., 1988. Evaluation of preliminary experiments assimilating Seasat significant wave heights into a spectral wave model. J. Geophys. Res., 93: 14,099–14,106.

De Las Heras, M. and Janssen, P.A.E.M., 1993. Wave data assimilation. In: The WAM wave model, Conference Data assimilation in Marine Science Liege, May, 1993.

Francis, P.E. and Stratton, R.A., 1990. Some experiments to investigate the assimilation of SEASAT altimeter wave height data into a global wave model. Q.J.R. Meteorol. Soc., 116: 1225–1251.

Goodberlet, M.A., Swift, C.T. and Wilkerson, J.C., 1992. Validation of the ocean surface wind fields and wave height measurements derived from data of the ERS-1 scatterometer and radar altimeter (early results). Workshop Proc. Penhors, France, 27–30 April 1992, ESA, pp. 36, 61–64.

Günther, H., Lionello, P. and Hansen, B., 1993. The Impact of the ERS-1 Altimeter on the Wave Analysis and Forecast. GKSS Scientific Center Rep., 93/E/44, 56 pp.

Janssen, P.A.E.M., Lionello, P., Reistad, M. and Hollingsworth, A., 1989. Hindcasts and data assimilation studies with the WAM model during the SEASAT period. J. Geophys. Res., 94: 973–993.

Hasselmann, K., Hasselmann, S., Bauer, E., Brüning, C., Lehner, S., Graber, H. and Lionello, P., 1988. Development of a satellite SAR Image Spectra and altimeter wave height data assimilation system for ERS-1. Max Planck Institut für Meteorologie Rep., 19, 155 pp.

Hasselmann, S., Brüning, C. and Lionello, P., 1993. Towards a generalized Optimal Interpolation Method for the assimilation of ERS-1 SAR retrieved wave spectra in a wave model. Second ERS-1 Symposium, Hamburg, October 1993.

Kitaigorodskii, S.A., 1962. Application of the Theory of Similarity to the Analysis of Wind-Generated Water Waves as a stochastic Process. Bull. Acad. Sci. USSR Geophys. Ser., 1, 73 pp.

Lionello, P. and Janssen, P.A.E.M., 1990. Assimilation of altimeter measurements to update swell spectra in wave models. In: Proc. Int. Symp. Assimilation of Observations in Meteorology and Oceanography. Clermond-Ferrand, France, August 1990, pp. 241–248.

Lionello, P., Günther, H. and Janssen, P.A.E.M., 1992. Assimilation of altimeter data in a global third generation wave model. J. Geophys. Res., 97(C9): 14,453–14,474.

Thomas, J., 1988. Retrieval of energy spectra from measured data for assimilation into a wave model. Q.J.R. Meteorol. Soc., 114: 781–800.

WAMDI group (S. Hasselmann, K. Hasselmann, E. Bauer, P.A.E.M. Janssen, G. Komen, L. Bertotti, P. Lionello, A. Guillaume, V.C. Cardone, J.A. Greenwood, M. Reistad, L. Zambresky and J.A. Ewing), 1988. The WAM model — A third generation ocean wave prediction model. J. Phys. Oceanogr., 18: 1776–1810.